Preparation and Characterization of a Biodegradable Polyester Elastomer with Thermal Processing Abilities

Quanyong Liu,[1] Ming Tian,[1,2] Tao Ding,[1] Rui Shi,[1] Liqun Zhang[1,2]

[1]*The Key Laboratory of Beijing City on Preparation and Processing of Novel Polymer Materials, Beijing University of Chemical Technology, Beijing 100029, People's Republic of China*
[2]*The Key Laboratory for Nano-materials, Ministry of Education, Beijing 100029, People's Republic of China*

Received 4 November 2004; accepted 9 February 2005
DOI 10.1002/app.22397
Published online in Wiley InterScience (www.interscience.wiley.com).

ABSTRACT: We studied the condensing reaction of sebacic acid and glycerol and prepared biodegradable elastomers. Swelling experiments proved that the elastomers were crosslinked polyesters consisting of both insoluble parts (gel) and soluble parts (sol), but the content of sol was higher than gel. X-ray diffraction analysis showed that some ordered and crystallized structures existed in most of the elastomers. Differential scanning calorimetry measurement showed that there were both crystal regions and amorphous regions with low glass-transition temperatures in the products, which indicated the elastomers had a microphase separation structure. The elastomers exhibited thermal processing abilities, such as mold-shaping performance, and a certain elasticity, and hydroxyl, carboxyl, and ester groups in the molecular chains endowed the elastomers with good biodegradation abilities. Furthermore, by altering the molar ratio of the reactants, we were able to adjust the mechanical properties, biodegradable performance, and so on of the elastomers. Glycerol and polymers containing sebacic acid have been approved for biological medical uses by the U.S. Food and Drug Administration, so the elastomers we prepared would have broad application in medical fields such as implants and drug-delivery systems. © 2005 Wiley Periodicals, Inc. J Appl Polym Sci 98: 2033–2041, 2005

Key words: biodegradable; elastomer; polyesters; processing

INTRODUCTION

Biodegradable polymers have been used widely in medical fields such as implants and drug-delivery systems.[1,2] In tissue engineering, for example, biodegradable polymers are used as scaffolds that sustain the attachment and growth of specific cells and greatly facilitate the generation of functional tissues.[3,4] Biodegradable elastomers can be tailored within wide ranges, which allows them to be used in many surgical applications in both soft and hard tissues because of their adjustable physical properties, especially their good flexibility.[5–9]

Biodegradable elastomers have usually been prepared as one of two types: thermoplastic elastomers or thermoset elastomers. Thermoplastic elastomers are usually phase-separated block copolymers[7,10,11] consisting of soft, rubber-like segments [with a low glass-transition temperature (T_g)], which impart flexibility to the materials, and glassy or crystallizable segments, which provide strength and stiffness by the formation of a hard phase; these include the segmented polyurethanes, poly(ethylene oxide) and poly(butylenes terephthalate), and segmented poly(ether ester amide). Thermoplastic elastomers have the advantage of being easily fabricated by melt processing. However, the crystallized hard regions these materials possess make their biodegradation slower and their remaining dimensions poor. Thermoset elastomers cannot not be shaped by melt processing, but the speed of biodegradation is more uniform, and the remaining dimensions are better. The following is a common synthesis method of thermoset elastomers. Star-shaped prepolymers are first gained by copolymerization and then crosslinked with degradable monomers such as lactide, glycolide, ε-caprolactone, δ-valerolactone, dioxanone, and trimethylene carbonate.[12–16] It is obvious that both thermoplastic elastomers and thermoset elastomers have advantages and disadvantages corresponding to their special structures and properties.[17–20]

Some researchers have prepared biodegradable thermoset elastomers by condensing glycerol and sebacic acid with molar ratio of 1/1 and found that the products had good flexibility, biocompatibility, and biodegradation properties.[19,21] To obtain the elastomers, they first synthesized a prepolymer and then poured an anhydrous 1,3-dioxolane solution of the prepolymer into a mold for curing and shaping under a high vacuum. Apparently, the final products could

Correspondence to: L. Zhang (zhangliqunghp@yahoo.com).

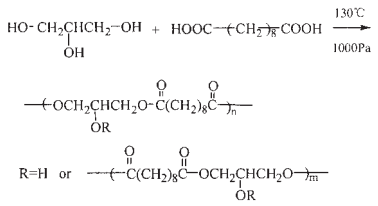

Scheme 1 Reaction formula for the condensing of glycerol and sebacic acid.

not be easily processed to their desired shape because of the lack of thermoplasticity.

Some authors have also conducted studies on the preparation of elastomers based on glycerol and sebacic acid and found that this kind of elastomer exhibited a certain thermal processing performance (e.g., shape-molding ability) in some molar ratios of glycerol to sebacic acid and under certain reaction conditions. Furthermore, the morphological structure, composition, and crystal degree of the elastomers greatly influenced their elasticity, strength, biodegradation, and thermal processing abilities. In another words, the properties of the elastomers could be flexibly adjusted by altering the molar ratio of the reactants. A specific and systemic report about these products has not yet been published.

EXPERIMENTAL

Materials

Glycerol (analytical grade) and dichloromethane (analytical grade) were obtained from Beijing Chemical Plant. Sebacic acid (chemical grade) was obtained from Shanghai Reagent Third Plant and was purified by recrystallization before use. Anhydrous ethanol (analytical grade) and tetrahydrofuran (analytical grade) were obtained from Beijing Century Red-Star Chemical, Ltd., Corp.

Synthesis of the elastomers

Glycerol and sebacic acid were mixed well at different molar ratios (glycerol/sebacic acid = 2/2, 2/2.5, 2/3, 2/3.5, and 2/4); then, these mixtures were added into a flask, heated until the monomers were completely melted, and stirred at 130°C under 1000 Pa. After about 23 h (ca. 48 h for the reaction with a molar ratio of 2/2), the reaction was stopped, and the products were cooled to room temperature. Nitrogen was constantly and slowly run into the flask during the whole process. The reaction formula[19] is shown in Scheme 1.

Processing of the elastomers

The synthesized elastomers were first hot-pressed into 1 mm thick sheets at 90°C under 15 MPa in a window mold; they were then transferred into another cold-press machine and molded at room temperature for 20 min (the products with a molar ratio 2/2 could not be mold-shaped by hot pressing).

Characterization of the elastomers

The IR spectra of the samples were recorded on a Nicolet-210 spectrophotometer with salt flake by hot casting for the structure information.

To investigate the reaction degree and the product compositions, a Bruker AV600 NMR spectrometer (Switzerland), which worked at 600.13 MHz for protons in acetone-d_6 with tetramethylsilane as a standard, was employed to determine the ^{1}H-NMR spectra of the products. The acetone-swollen sample was tested with high-resolution/magic-angle spinning.

The sol content of the products and the swelling degree (R) of the corresponding gels were measured in the following way.[20] A small disc sample (1 mm in thickness and 10 mm in diameter) with weight W_1 was dipped in 40 mL of dichloromethane for 24 h and was then taken out and dried to a constant weight W_2 in a vacuum oven at 40°C under 4000 Pa. The sol content was calculated as follows: $Q_1 = (W_1 - W_2)/W_1 \times 100\%$. Another small disc sample with weight H_1 was dipped in 40 mL of tetrahydrofuran for 24 h and was then taken out. We recorded the weight of the disk as H_2 after the solvent on its surface was absorbed by filter paper and then dried the disk to a constant weight H_3 in a vacuum oven at 40°C under 4000 Pa. The sol content was calculated as $Q_2 = (H_1 - H_3)/H_1 \times 100\%$, and R of the corresponding gel was calculated as $R = (H_2 - H_3)/H_3 \times 100\%$. Three samples were taken for each experiment, and the average value of three samples is reported.

The equilibrium water uptake in deionized water was defined as the fraction of gained weight of a small disc sample and was calculated as Water uptake $= (M_2 - M_1)/M_1 \times 100\%$, where M_1 is the initial weight of the specimen and M_2 is the weight of the sample after it was dipped in deionized water for 24 h. Three samples were tested for each product at room temperature, and the average value was obtained.

The specimens for mechanical testing were cut from the 1 mm thick samples according to ISO/DIS 37-1990 type 3 specifications (dumbbell-shaped specimens, width = 2 mm). Tensile tests were performed in a universal tensile testing machine equipped with a 500-N load cell operated at a crosshead speed of 10 mm/min. The specimen's elongation was derived from an extensometer separation of 20 mm. The elastic modulus (E) was determined from the initial slope of the stress–strain curve (1–5% strain range of the stress–strain curve). Three samples of each product were tested at 23°C.

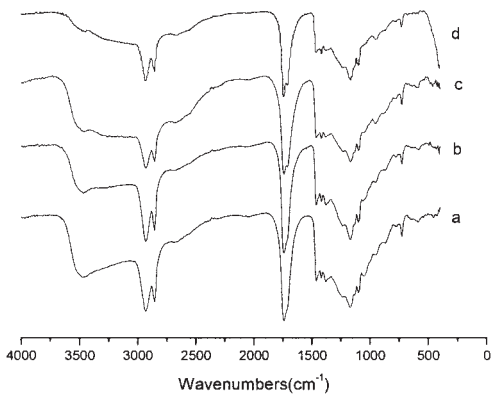

Figure 1 IR spectra of the products with molar ratios of (a) 2/2.5, (b) 2/2, (c) 2/3, and (d) 2/4.

The wide-angle X-ray diffraction (XRD) patterns of products were recorded with a Rigaku model D/Max2500VB2+/PC X-ray diffractometer (Japan) with nickel-filtered Cu Kα radiation with a 1 mm thick sheet with a smooth surface.

The thermal properties of the original products (composed of gel and sol) and their corresponding gel parts (which we obtained by dipping the products in tetrahydrofuran for 24 h and then drying them to a constant weight in a vacuum oven at 40°C under 4000 Pa) were evaluated by differential scanning calorimeter (PerkinElmer) at a heating and cooling rate of 10°C/min. The sample (17–20 mg) was placed in aluminum pan and was first heated from 40 to 150°C and held there for 5 min to remove its heating history; then, the cooling scan was recorded from 150 to −120°C. Subsequently, a second heating scan was conducted from −120 to 150°C. The T_g values were taken as the midpoint of the heat-capacity change, and the melting temperature (T_m) and crystallization temperature (T_c) were determined from the maximum in the melting endotherm and the crystallization exotherm, respectively.

The hydrophilicity of products was characterized by measurement of the water-in-air contact angle of the smooth surfaces of 1 mm thick samples through with a Germany Dataphysics OCA20 water contact angle measurement instrument. The sessile drop method was adopted, and the results are the average of five values.

In vitro degradation study

The small disc samples (10 mm in diameter and 1 mm in thickness) cut from the 1 mm thick sheet were used for the *in vitro* degradation study. Here, we mainly considered hydrolysis degradation. A sample with weight G_1 was put into a taper bottle and immersed in a 37°C phosphate buffered saline (PBS) solution (pH = 7.4). The PBS was replaced every 36 h to ensure a constant pH of 7.4. Samples were taken out after a certain time and washed three times with deionized water and were then dried to a constant weight G_2 in a vacuum oven at 40°C under 4000 Pa. The mass loss was calculated as follows: Mass loss = $(G_1 - G_2)/G1 \times 100\%$. Three samples for each product were tested to achieve an average value.

RESULTS AND DISCUSSION

IR analysis

IR (cm^{-1}): 1740 (ν C═O ester), 1700 (ν C═O carboxyl), 3460 (ν OH).

As shown by the IR spectra (Fig. 1), the absorption peak of hydroxyl groups was wide and shifted to a low wave number, which demonstrated the existence of hydrogen-bonding action. The absorption of hydroxyl groups was weakened, whereas the absorption of carboxyl carbonyl was strengthened with the increase of sebacic acid in the reaction. That means, when more sebacic acid was used, the esterification degree of glycerol improved, and the number of residual hydroxyl groups decreased, although the increasing of number of carboxyl carbonyl groups was attributed mostly to the increasing number of carboxyl groups at the molecular chain ends of the final products.

^{1}H-NMR spectra

The peaks of the ^{1}H-NMR spectra of products were classified[22–24] as follows (Fig. 2 only presents the spectrum of the products with a molar ratio of 2/3.5 because the spectra of the other products were similar). The hydrogen protons of the hydroxyl groups in the products were exchanged with D_2O; however, little influence of them was found in the results. So the area

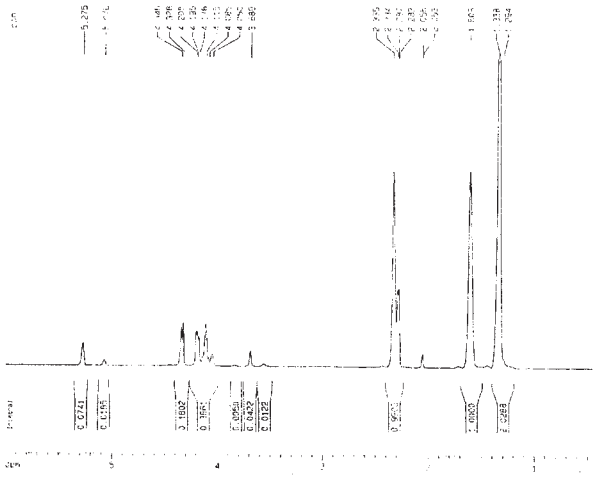

Figure 2 ^{1}H-NMR spectra of the product with a molar ratio of 2/3.5.

TABLE I
^{1}H-NMR Analysis of the Products

Molar ratio	Actual molar ratio	Esterification degree		Molar percentage of residual —OH (%)
		—CH_2—OH (%)	—CH—OH (%)	
2/2.5	2/2.59	61.88	16.07	22.05
2/3	2/2.85	63.69	18.57	17.74
2/3.5	2/3.49	65.70	21.48	12.82
2/4	2/3.72	65.89	22.18	11.93

of different peaks was calculated directly without consideration of the influence of the hydrogen protons of the hydroxyl groups. The actual molar ratio (F) of the reactants, the esterification degree of hydroxyl groups, and the percentage of residue hydroxyl groups were obtained according to the following formula, and all of the final results are listed in Table I:

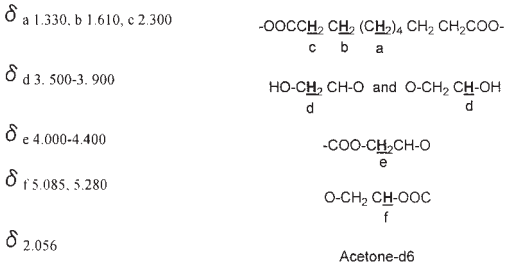

S is the area of peak, δ is the chemical shift (ppm), and a, b, c, d, e, and f are the categories of hydrogen protons. F (glycerol/sebacic acid) was equal to $16S_{\delta\text{-d,e,f}}/5S_{\delta\text{-a,b,c}}$. The esterification degree of —CH_2—OH (1 mol of glycerol) was calculated as $E_1 = 5S_{\delta\text{-e}}/6S_{\delta\text{-d,e,f.}}$ The esterification degree of —CH—OH (1 mol of glycerol) was calculated as $E_2 = 5S_{\delta\text{-f}}/3S_{\delta\text{-d,e,f}}$ The percentage of residual hydroxyl groups (1 mol of glycerol) was calculated as $Q = 1 - E_1 - E_2$.

In theory (^{1}H-NMR analysis), the maximum esterification degree of —CH_2—OH was 66.67% (2/3), and the maximum esterification degree of —CH—OH was 33.33% (1/3). As shown in Table I, the actual esterification degrees of two kinds of hydroxyl groups in the final products were lower than the theoretical values, which indicated that residue hydroxyl groups existed.

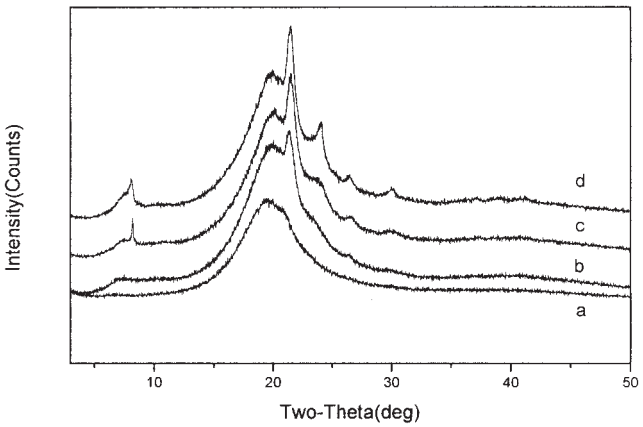

Figure 3 XRD curves of the products with molar ratios of (a) 2/2.5, (b) 2/3, (c) 2/3.5, and (d) 2/4.

Furthermore, the difference between the experimental esterification degree and the theoretical esterification degree of —CH_2—OH was much smaller than that of —CH—OH, which apparently ascribed to the lower esterification reaction activity of —CH—OH, which was probably caused by a bigger steric hindrance effect. Table I also clearly illustrates that the esterification degree of glycerol —OH became higher and higher with increasing sebacic acid content.

Swelling properties, structures of the sol and gel products, and water-uptake performances

The sol content, R, water uptake, and the mechanical properties [tensile strength (δ), E, and elongation at break (ε)] of the elastomers are summarized in Table II. At first, we found that the difference in the sol contents Q_1 and Q_2 was remarkable, which was attributed to the fact that the products could be swollen better and their corresponding sol parts could be dissolved better in tetrahydrofuran than in dichloromethane. During swelling, the sol part of the product dissolves out from the products in tetrahydrofuran at maximum, so it is more accurate to measure the sol content and R of the gel part of the products with tetrahydrofuran as a solvent. As shown in Table II, Q_1 and Q_2 of the product with a molar ratio of 2/3.5 were

TABLE II
Sol Contents, R, Water Uptake, and Mechanical Properties of Products

Molar ratio	Q_1 (%)	Q_2 (%)	R (%)	Water uptake (%)	δ (MPa)	E (MPa)	ε (%)
2/2.5	29.72	75.13	3722.76	3.83	0.2104	0.0725	114.48
2/3	35.45	74.81	3447.20	5.43	0.1409	0.1347	101.32
2/3.5	22.63	69.23	2742.98	4.32	0.6990	1.4510	57.22
2/4	27.18	84.23	5188.18	7.28	0.4253	7.0527	12.00

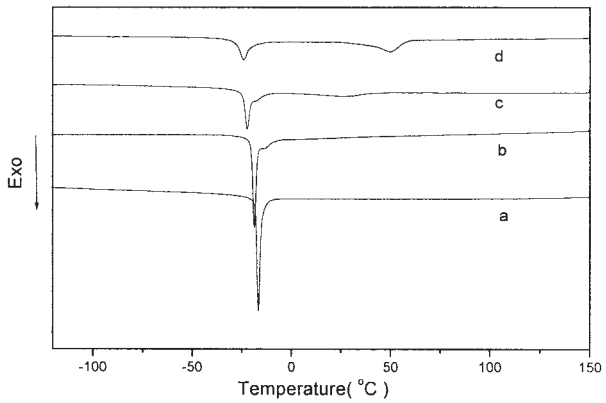

Figure 4 DSC crystallization curves of the products with molar ratios of (a) 2/2.5, (b) 2/3, (c) 2/3.5, and (d) 2/4.

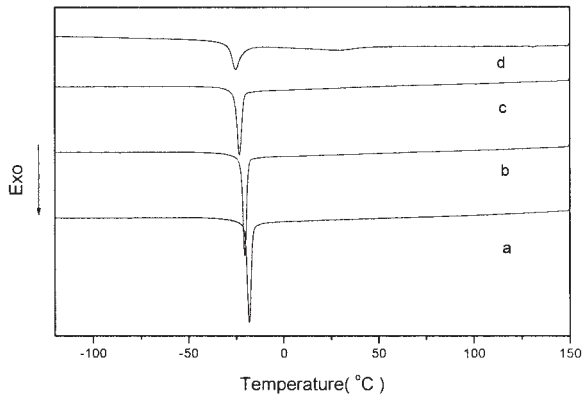

Figure 6 DSC crystallization curves of the gel parts of the products with molar ratios of (a) 2/2.5, (b) 2/3, (c) 2/3.5, and (d) 2/4.

the lowest, which implied that the gel content of these products was the highest, whereas Q_2 of the product with a molar ratio of 2/4 was the highest, which indicated that the gel content of the 2/4 product was the lowest. In short, the gel parts of the products gradually increased with increasing sebacic acid content in the system until the molar ratio of the reactants reached 2/3.5. Considering the mechanism of condensing polymerization, the previous regulation was easily understood. With the decreasing molar ratio of the reactants, more and more hydroxyl groups located in the chain and chain end of the precopolymer were esterified by sebacic acid, which was strongly proven by ^{1}H-NMR, as shown in Table I. As a result, on the one hand, more crosslinking points could be formed due to the three-functional-group structure of glycerol, and on the other hand, more sol parts with a certain molecular weight could be produced due to the loss of reaction ability when hydroxyl groups transformed into acid groups. These two effects competed in the reaction, and the former gained the advantage before the molar ratio reached 2/3.5, whereas the latter exerted a main effect when the molar ratio reached 2/4.

R of elastomers is an important method for characterizing the crosslinking degree of elastomers. From the *R* values of the products shown in Table II, two interesting phenomena are worth discussing. First, all of the swelling percentage values reached several thousands, which implied that the crosslinking degree of products, more precisely, the gel parts, was very low. Second, the *R* values of the products first decreased and reached their lowest values with decreasing molar ratio and then went up when the molar ratio passed 2/3.5. Furthermore, *R* reached its highest value when the molar ratio was 2/4. To explain this swelling behavior of the products with the molar ratio of the reactants, we suggest that the structure of the polyester elastomers we synthesized was a semi-interpenetrated network structure where branched and liner polyester macromolecules existed in crosslinked polyester networks and penetrated through the networks. On the basis of such a structure model, the *R* value of

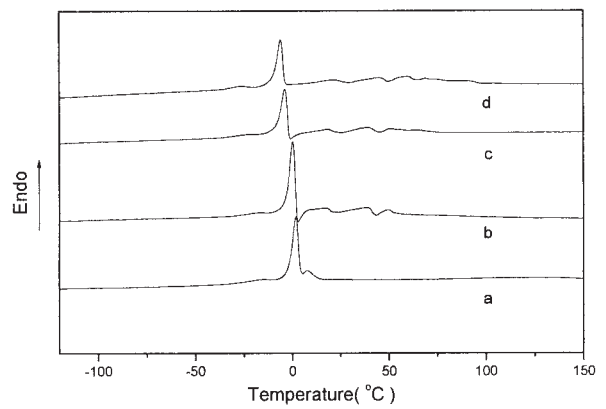

Figure 5 DSC melting curves of the products with molar ratios of (a) 2/2.5, (b) 2/3, (c) 2/3.5, and (d) 2/4.

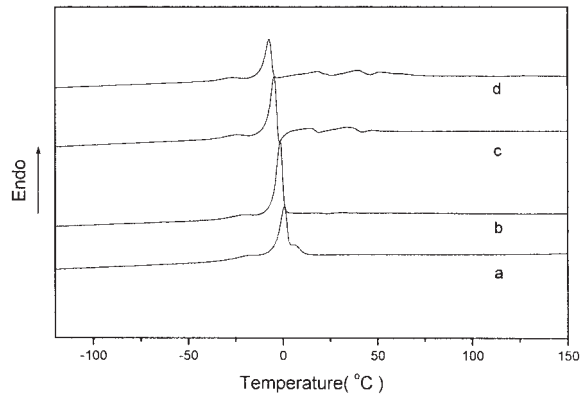

Figure 7 DSC melting curves of the gel parts of the products with molar ratios of (a) 2/2.5, (b) 2/3, (c) 2/3.5, and (d) 2/4.

TABLE III
DSC Results of the Products (Sol and Gel)

Molar ratio	T_g (°C)		T_m (°C)			T_c (°C)		ΔH (J/g)	
2/2.5	−25.1	1.8	7.5	—	—	−16.8	—	−44.17	—
2/3	−27.1	0.2	8.4	39.2	49.6	−18.8	—	−39.45	—
2/3.5	−29.9	−3.8	17.3	39.3	51.2	−22.4	25.7	−28.17	−12.96
2/4	−32.2	−5.9	20.9	44.9	59.6	−24.2	49.8	−19.96	−22.38

the products would be related to both sol swelling and gel swelling. Therefore, for the product with a molar ratio of 2/4, although the crosslinking density of gel parts was believed to increase with decreasing molar ratio according to the ^{1}H-NMR results, which benefited the decrease of R, the rapid increase of the sol content of the product with a molar ratio of 2/4 led to a great increase in R, which gained an advantage over the crosslinking. This regulation was still ascribed to the competition effect existing in the condensing polymerization of glycerol and sebacic acid, which was mentioned previously.

The water uptake of the products presented in Table II was not high; this was because the water was prevented from diffusing into the materials by the presence of a crosslinking structure and crystallization regions of the products, which is illustrated in the following section.

Crystallization properties

XRD curves of the products with different molar ratios are displayed in Figure 3. The XRD curve of the product with a molar ratio of 2/2.5 mainly showed three broad peaks (6.764, 19.581, and 40.640°), whereas the other curves showed more distinct peaks in addition to these three peaks. At the same time, the intensity of these peaks became stronger and stronger with increasing sebacic acid. All these suggest the existence and strengthening of crystal regions in the products with molar ratios of 2/3, 2/3.5, and 2/4. The intensified ordered structure came from the improved regular networks.[25,26] However, the XRD results could not distinguish between the contributions to crystallization of the gel parts and the sol parts.

The differential scanning calorimetry (DSC) melting and crystallization curves of the products with different molar ratios and the corresponding gel parts extracted from the products were investigated and are shown in Figures 4–7. Tables III and IV sum up the T_g, T_m, T_c, and crystallization enthalpy (ΔH) data for all of the products and gels. As shown, for each product, a distinct crystallization and melting peak existed. However, this distinct crystallization definitely disappeared below room temperature due to the lower T_m. As a result, this obviously did not affect the mechanical properties, biodegradable properties, surface properties, and thermal processing performance of the products, and it was not reflected in the XRD experiments carried out at room temperature. Table III and the corresponding DSC curves also show that the product with a molar ratio of 2/2.5 had only one T_c (−16.8°C) and two T_m's that were below room temperature, whereas the products of with molar ratios of 2/3, 2/3.5, and 2/4 showed crystallization behavior both below and above 0°C, especially for the products with molar ratios of 2/3.5 and 2/4. The products with molar ratios of 2/3, 2/3.5, and 2/4 also displayed other T_m's that were higher than room temperature. These results were in accordance with XRD analysis, which implied that the crystallization of the products that survived at room temperature originated from an ordered structure with a higher T_m than room temperature. Moreover, from the DSC melting curves of the products, it was shown that with decreasing molar ratio, the total melting enthalpy of the products above room temperature increased, which was also consistent with the XRD results. When the enthalpy of these crystallizations at high temperature were compared with that of a distinct crystallization at lower temperature, we also deduced that the crystallization degree of the products at room temperature was low. The low crystallinity is extremely important for good elasticity in an elastomer.

The crystallization and melting of the gel parts are shown in Figures 6 and 7. When we compared the

TABLE IV
DSC Results of the Gel Parts of the Products

Molar ratio	T_g (°C)		T_m (°C)			T_c (°C)		ΔH (J/g)	
2/2.5	−25.3	0.7	7.5	—	—	−18.2	—	−39.69	—
2/3	−27.9	−1.5	32.3	—	—	−20.7	—	−34.92	—
2/3.5	−30.7	−4.6	5.8	34.1	47.4	−23.4	—	−28.57	—
2/4	−33.4	−7.3	18.2	39.9	51.3	−25.4	28.7	−20.54	−11.03

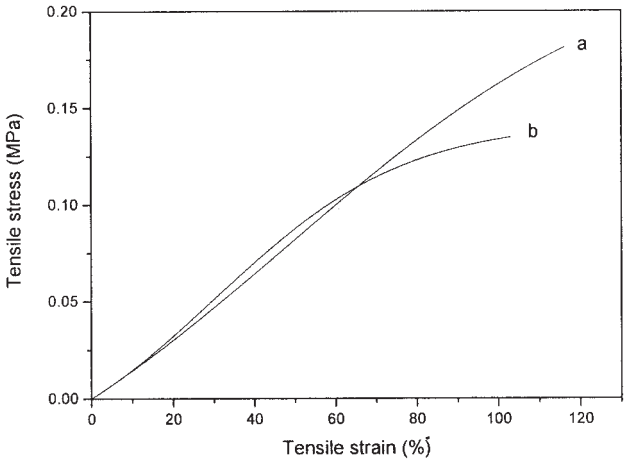

Figure 8 Stress–strain curves of the products with molar ratios of (a) 2/2.5 and (b) 2/3.

results of the products (sol and gel), we were able to draw some conclusions. First, the gel parts of the products could crystallize, their crystallization characteristics and melting properties were pretty similar to that of the products, and their ΔH's were smaller but close to that of product, which implied that the crystallization of the gel was mainly responsible for the crystallization of the product. Second, the T_c of the gel parts at a lower temperature gradually decreased and ΔH gradually decreased with decreasing molar ratio, which was probably caused by the increase in the crosslinking density and branching degree of gel. Third, the T_m range of the gel parts expanded and extended to a higher temperature with decreasing molar ratio, and for the product with a 2/4 molar ratio, there were two distinct T_c existed, which was hard to understand. Some authors have assumed that there are many kinds of ordered structures in the gel and products[27] that possess different crystallization and melt behaviors. With decreasing molar ratio, the crosslinking degree and esterification degree of the gel increased, and a series of macromolecules with different but poor thermal motion abilities (i.e., high stiffness) arose, which further assembled and stacked to form many kinds of ordered microregions (i.e., crystal regions). As a result, a complex melting region in the DSC curves and higher T_m came into being. More detailed research on the crystallization of this kind of polyester elastomer should be conducted.

The presence of crystallization in the polyester elastomer endowed it with a good thermal processing performance. Through the melting and reforming of crystallization, the elastomer could be molded into the desired shape at high temperatures, and the shape could be kept stable at room temperature, which was proved by our molding experiments.

Glass transition

In Tables III and IV, the T_g values derived from DSC curves of the products with different molar ratios are summarized. The T_g's of all of the products and gels were much lower than room temperature, which guaranteed the necessary elasticity for this kind of materials. In addition to decreasing molar ratio, the T_g's of all of the products and gels became lower and lower. This was probably due to the effect of crystallization that occurred at lower temperatures. Specifically, with decreasing molar ratio, the low-temperature crystallization decreased, and its confinement to the macromolecules located in amorphous region weakened. The coexistence of the crystal region and the amorphous regions in the products resulted in microphase separation structure, which was probably a useful morphology, serving as anticoagulant materials such as polyurethane.

Mechanical properties

The mechanical properties of all the products are listed in Table II; the E values of the products increased all the time with decreasing molar ratio; correspondingly, ε of the products decreased monotonously. δ of products with different molar ratio showed a trend of first increasing and then decreasing. The stress–strain curves of the products are shown in Figures 8 and 9. With decreasing molar ratio of the reactants, the crosslinking density of the products roses, and the crystallinity above room temperature also increased; the combination effect led to an increase in E, a decrease in ε, and a possible increase in δ. However, with decreasing molar ratio of the reactants, the sol content of the products first decreased and then increased. The sol content was thought to be harmful to δ and E. Hence, the mechanical properties

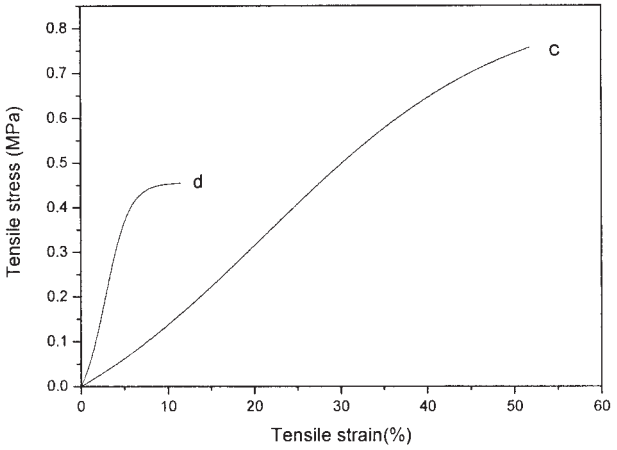

Figure 9 Stress–strain curves of the products with molar ratios of (c) 2/3 and (d) 2/4.

were the comprehensive result of the sol content, crystallinity, and crosslinking degree of elastomer. In other words, through adjustment of the molar ratio of the reactants and the relative reaction conditions, the complex chemical structure and phase structure of the elastomers could be flexibly adjusted to fabricate different biomedical products.

Surface properties

The water-in-air contact angle data of the products are displayed in Table V. Generally speaking, all of the products were hydrophilic because of the existence of hydroxyl groups, carboxyl groups, and ester groups in the molecular chains. Table V also illustrates that the contact angle increased with decreasing molar ratio, which indicated that the hydrophilicity of the products was weakened. It is well known that glycerol is hydrophilic due to its three hydroxyl groups, whereas sebacic acid with long alkyl chains only shows a certain hydrophilicity. So the hydrophilicity of the products was partly adjustable by a change in the molar ratio of glycerol to sebacic acid, which actually changed the esterification degree of the glycerol hydroxyl groups.

In vitro degradation properties

Figure 10 shows the mass loss–time curves of the products with different molar ratios in a 37°C PBS solution (pH = 7.4), which characterized the *in vitro* degradation of the products. Generally speaking, the hydrolytic mechanism of materials involves bulk degradation and surface degradation. The products synthesized in this study were mostly composed of sol, so their degradation mainly corresponded to the degradation of sol parts, but the degradation of sol was definitely restricted by the networks and crystallization of the gel. As shown by the degradation curves, the mass loss of products with different molar ratios was fast and about 10% after the first 1.5 days and then became slow and stable in the latter period. The fast degradation occurring in former period might have been caused by the quick degradation of sol with low molecular weight. Among the four products with different molar ratios, the degradation speed of the products with a 2/2.5 molar ratio was the slowest, which was mainly ascribed to its higher average molecular weigh of sol parts, whereas the degradation speed of the 2/4 product was the fastest due to its highest sol content and lower average molecular weigh of sol parts. By observing the degradation phenomenon of the products, we found that the dimension of the products was gradually reduced, and less visible bulks of samples were found, which demonstrated that the degradation of products mainly behaved as a surface degradation, which was related to its low water uptake and a certain crosslinking structure.

TABLE V
Water-in-Air Contact Angles of the Products

Molar ratio	2/2.5	2/3	2/3.5	2/4
Contact angle (°)	45.2	47.9	52.3	56.6

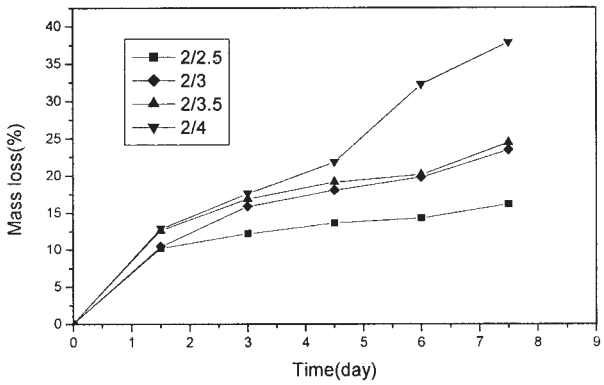

Figure 10 *In vitro* degradation mass loss–time curves of the products.

CONCLUSIONS

The biodegradable elastomer synthesized by condensing glycerol and sebacic acid in this study was actually a polyester network, which was composed of a high sol content and a low gel content and was partly thermoplastic. The elastomer held a microphase separation structure formed by soft amorphous regions and hard crystal regions. Soft regions with lower T_g values endowed the elastomer with flexibility, and hard regions provided strength, stiffness, and a certain thermal processing ability. We suggest that the sol parts and gel parts formed a semi-interpenetrated network. The molar ratio of the reactants greatly influenced the chemical structure, phase structure, and ratio of sol to gel of the products and further affected the properties of the products. The elastomer had good *in vitro* biodegradation performance and a certain elasticity, and the properties of products could be flexibly adjusted by the alteration of the molar ratio.

References

1. Kazuhiko, H.; Mie, S.; Takayuki, S.; Yoshiki, I. J Appl Polym Sci 2004, 92, 3492.
2. Yu, L.; Li Kun, G.; Long, H.; Xian Mo, D. J Appl Polym Sci 2003, 90, 3150.
3. Engelmayr, G. C.; Hildebrand, D. K.; Sutherland, F. W. H. Biomaterials 2003, 24, 2523.
4. Calandrelli, L.; Immirzi, B.; Malinconico, M.; Volpe, M. G.; Oliva, A.; Della Ragione, F. Polymer 2000, 4, 8027.
5. Peppas, N. A.; Langer, R. Science 1994, 263, 1715.

6. Pathiraja, A. G.; Raju, A. Eur Cells Mater 2003, 5, 1.
7. Deschamps, A. A.; Grijpma, D. W.; Feijen, J. J Biomater Sci Polym Ed 2002, 12, 1337.
8. Mulder, M. M.; Hitchcock, R. W.; Tresco, P. A. J Biomater Sci Polym Ed 1998, 9, 731.
9. De Groot, J. H.; Spaans, C. J.; Dekens, F. G.; Pennings, A. J Polym Bull 1998, 41, 299.
10. Deschamps, A. A.; Grijpma, D. W.; Feijen, J. Polymer 2001, 42, 9335.
11. Fakirov, S.; Goranov, K.; Bosvelieva, E.; Du Chesne, A. Makromol Chem 1992, 193, 2391.
12. Graessley, W. W.; Roovers, J. Macromolecules 1979, 12, 959.
13. Meidong, L.; Renee, P. W.; Chih-Chang, C. J Polym Sci 2002, 40, 1127.
14. Michael, A.; Carnahan, M. W. G. J Am Chem Soc 2001, 123, 2905.
15. Minoru, N.; Tetsuya, M.; Wataru. S.; Naoto, T. J Polym Sci 1999, 37, 2005.
16. Robson, F.; Storey, S. C.; Warren, C. J. A.; Puckett, A. D. Polymer 1997, 26, 6295.
17. Kylma, J.; Seppala, J. Macromolecules 1997, 30, 2876.
18. Dahiyat, B. I.; Posadas, E. M.; Hirosue, S.; Hostin, E.; Leong, K. W. React Polym 1995, 25, 101.
19. Wang, T.; Ameer, G. A.; Sheppard, B. J.; Langer, R. Nat Biotechnol 2002, 20, 602.
20. Storey, R. F.; Hickey, T. P. Polymer 1994, 35, 830.
21. Yadong, W.; Yu, M. K.; Robert, L. J Biomed Mater Res A 2003, 66, 192.
22. Meidong, L.; Renee, P. W.; Chih-Chang, C. J Polym Sci Part A: Polym Chem 2002, 40, 1127.
23. Nuria, G.; Julio, G.; Evaristo, R. Macromol Chem Phys 2002, 203, 2225.
24. Steffen, M.; Alexander, S.; Holger, F.; Rolf, M. Macromol Rapid Commun 2000, 21, 226.
25. Tsuyoshi, K.; Nobuhisa, T.; Naoto, T.; Wataru, S. Polym Int 1996, 40, 17.
26. Minru, N.; Tetsuya, M.; Wataru, S.; Naoto, T. J Polym Sci Part A: Polym Chem 1998, 37, 2005.
27. Guangming, Z. Shape Memory Polymer and Application; Chemical Industry Press: Beijing, 2002; p 178.